Journal of Civil Engineering and Environmental Technology
p-ISSN: 2349-8404; e-ISSN: 2349-879X; Volume 3, Issue 5; April-June, 2016, pp. 399-405

http://www.krishisanskriti.org/Publication.html

Strengthening of Semi-Compact HSS Tubular Members using CFRP Composites

M. Priyadarshni[1] and M.C. Sundarraja[2]

[1]*PG Student, Department of Civil Engineering Thiagarajar College Of Engineering Madurai, India*
[2]*Department of Civil Engineering Thiagarajar College Of Engineering Madurai, India*
E-mail: [1]priyadarshni915@gmail.com, [2]mcsciv@tce.edu

Abstract—*The hollow steel sections (HSS) with tubular shape show the excellent properties with regard to loading in compression, torsion and bending in all directions. Though with the advantages of this type of structural members, they associated with certain drawbacks such as the susceptibility to local buckling loads, which may result in significant reduction of load-carrying capacity and functional capability. The studies on enhancing the behavior of such structures have significantly increased recently. The conventional methods of repairing or strengthening of these tubular structures are in existence, but they are associated with many disadvantages. The application of fibre reinforced polymer for strengthening steel structures might be a promising alternative because of their high tensile strength, low weight, high strength to weight ratios and excellent resistance to corrosion. The present investigation has been carried out to study the axial behaviour of short semi compact HSS tubular members (class3) externally bonded with the carbon fibre reinforced polymer (CFRP) composites both experimentally and analytically. The design strength equations were developed, based on various standards and codes. The axial compression tests were also carried out on ten numbers of externally CFRP strengthened short steel circular hollow sections. Finally, the analytical results were evaluated by comparing with the experimental results.*

1. INTRODUCTION

Steel plays an important role in civil industry. Varieties of steel sections are available. Among these sections, the hollow structural sections (HSS) are the most reliable one [8] and are of more importance than for steel structures of open sections. The HSS with tubular shape show the excellent properties with regard to loading in compression, torsion and bending in all directions. The closed shape without sharp corners reduces the area to be protected and extends the corrosion protection life [10]. The circular hollow section (CHS) often offers a decisive advantage with regard to structure exposed to air or water flow. Though with the advantages of this type of structural members, they are associated with some drawbacks such as susceptibility of HSS tubular structures to local buckling loads, which may result in significant reduction of load-carrying capacity and functional capability.

The studies on enhancing structures have significantly increased recently. A large number of steel structures, such as buildings, offshore platforms, large mining equipment and bridges get damaged due to various reasons e.g. design fault, material degradation, and change in the load acting on the structures. The conventional method of repairing or strengthening steel structures is to cut the damaged portion and replace it with plating, or attach external steel plates to the damaged portion of the member. These plates are usually bulky, heavy, difficult to fix and prone to corrosion. Also, the retrofitting using steel plates has some disadvantages like use of heavy lifting equipment to lift the plates and, due to this, additional dead load will be on the structure. So there is a need to look for alternatives[4].

Many studies have been conducted on repair and strengthening of structures using advanced composites. The fibre-reinforced polymer (FRP) has great advantages as a structural material, which restores the capacity of damaged structures. The application of carbon fibre reinforced polymer (CFRP) fabrics for strengthening steel structures might be a promising alternative because of their high tensile strength, low weight, high strength to weight ratios and excellent resistance to corrosion. The cost of repairing or retrofitting of steel structures with FRP composites far less than replacement and takes less time for construction, and the service interruption time can also be reduced. Hence the use of FRP appears to be an excellent solution.

Lelli Van Den Einde, Lei Zhao and Frieder Seible [5] studied the application of FRP in the renewal of constructed facilities infrastructure such as buildings, bridges, pipelines, etc. Recently, the use of FRP has been increased in the rehabilitation of concrete structures, mainly due to their tailorable performance characteristics, ease of application and low life cycle costs. These characteristics and the success of structural rehabilitation measures have led to the development of new lightweight structural concepts utilizing all FRP systems or new FRP/concrete composite systems. Their paper presented an overview of the research and development of applications of advanced composites to renewal of civil infrastructure at the University of California, San Diego (UCSD).

Mina Dawood, Emmett Sumner and Sami Rizkalla [6] investigated the use of carbon fibre reinforced polymer for strengthening steel bridges and structures. This paper described the details of an experimental program, which was conducted to investigate the fundamental behavior of steel-concrete composite bridge girders strengthened with high modulus (HM) CFRP materials. The behavior of the beams under overloading and fatigue loading conditions as well as the possible presence of a shear lag effect between the steel beam and the CFRP strengthening was studied. The flexural design guidelines are presented which can be used to establish the allowable live load increase for a strengthened beam and to design the required HM CFRP strengthening.

Viveka V., Shanmugavalli B. and Sundarraja M.C. [9] investigated the feasibility of strengthening circular hollow steel tubular sections subjected to compression and developed or predicted the suitable wrapping scheme of FRP to enhance the structural behaviour of it. Mild steel tubes with varying D/t ratio were considered with the main variable being FRP characteristics. Analytical investigation has been done to predict the axial compressive strength of circular hollow steel tubes strengthened with CFRP as per the recommendations of various codes and standards. Evaluation of their results lead to optimum FRP jacketing/wrapping arrangements for the steel tubes they have considered.

Jagtap P.R., Pore S.M. and Vipul Prakash [4] reviewed the available design guidelines for the selection, design and installation of FRP systems for external strengthening of steel structures. Various types of FRP plates, with their properties such as high strength to weight ratio and good resistance to corrosion, represented an ideal material in external retrofitting. They concluded that due to the promising performance and other advantages of bonding FRP laminates to steel structures, this technique is becoming increasingly popular. If the cost constraint is kept aside, the fiber wrapping system proves to be advantages over conventional strengthening processes. As the economy is moving ahead and infrastructure development is catching its pace, demand for fiber reinforced polymer in civil construction, which is slowly increasing and becoming acceptable.

An overview of past research on application of composites in rehabilitating deficient civil engineering structures and also the various studies carried out on FRP strengthened hollow structural steel (HSS) members indicated that there is a great potential for using CFRP to upgrade hollow steel tubular structures. The present investigation has been carried out to study the axial behaviour of semi-compact (class 3) HSS tubular members externally bonded with the CFRP strips both analytically[7] and experimentally.

2. ANALYTICAL INVESTIGATION[7]

2.1 Australian/New Zealand Standard 4600 [2]

Plate slenderness ratio for circular hollow steel tubular sections (λ) is given by the equation (1). The elastic buckling coefficient (k) was taken as 4.0 for stiffened elements. The elastic buckling stress (f_{crs}) is given by the equation (2). The equations (1) and (2) are applicable only to plain steel columns and they are used to predict the ultimate load carrying capacity of plain steel columns.

$$\lambda_s = \sqrt{\frac{f_y}{f_{crs}}} \quad (1)$$

$$f_{crs} = \frac{k\pi^2 E_s}{12(1-\nu^2)}\left(\frac{t_s}{d_i}\right)^2 \quad (2)$$

By knowing the values of elastic buckling stress and plate slenderness ratio, the ultimate load carrying capacity of the plain steel section (P_{us}) can be predicted through the following equations (3) and (4).

$$\rho_s = \frac{1-\frac{0.22}{\lambda_s}}{\lambda_s} \quad (3)$$

$$P_u = \rho_s A_s f_{ys} \quad (4)$$

The concept of modular ratio is applied for modifying the above four equations to calculate the axial capacity of CFRP strengthened steel tubular short columns. The thickness of each carbon layer was assumed to be uniform and the bond between the CFRP and the steel are to be adequate. The total thickness of the steel and supplanted area from steel to CFRP is calculated as

$$t_t = t_s + t_{cfrp} + t_a \quad (5)$$

where t_s – thickness of the steel section; t_{cfrp} – thickness of carbon fibre; t_a – thickness of adhesive.

The equivalent elastic modulus of CFRP can be determined by equation (6), where the nominal values of carbon fibre modulus (E_{cf}) and the adhesive modulus (E_a) of 240 GPa and 1.9 GPa, respectively were used. To calculate the elastic buckling stress for CFRP strengthened section, the transformed flexural rigidity (D_t) was used.

$$E_{cfrp} = \frac{E_a t_a + E_{cf} t_{cf}}{t_a + t_{cf}} \quad (6)$$

$$D_t = \frac{AC - B^2}{A} \quad (7)$$

where,

$$A = \frac{E_s}{1-\nu_s^2} t_s + \frac{E_{cfrp}}{1-\nu_{cf}^2}(t_t - t_s)$$

$$B = \frac{E_s}{1-\nu_s^2}\frac{t_s^2}{2} + \frac{E_{cfrp}}{1-\nu_{cf}^2}\frac{(t_t^2 - t_s^2)}{2}$$

$$C = \frac{E_s}{1-\nu_s^2}\frac{t_s^3}{3} + \frac{E_{cfrp}}{1-\nu_{cf}^2}\frac{(t_t^3 - t_s^3)}{3}$$

With the above transformations the equations (1) to (4) can be modified for the case of strengthened steel columns as follows,

$$f_{crc} = \frac{k\pi^2}{t_t d_i^2} D_t \quad (8)$$

$$\lambda_c = \sqrt{\frac{f_y}{f_{crc}}} \quad (9)$$

$$\rho_c = \frac{1 - \frac{0.22}{\lambda_c}}{\lambda_c} \quad (10)$$

$P_{uc} = \rho_s A_s f_{ys} + \rho_c A_{cfrp} f_{cfrp}$ (11)

where $A_{cfrp} = A_r + A_{frp}$; A_r – area of resin; A_{frp} – area of carbon fibre. The predicted strength values are presented in Table 1.

2.2 European standard EN 1993-1-1 (2005) [3]

This standard classifies steel sections as class 1, 2, 3 and 4. Cross sections with $(D_s/t_s) \le 90\varepsilon^2$, where $\varepsilon = \sqrt{235/\sigma_y^s}$, are classified as class 1, 2 and 3. In this study, the sections considered fall under (D_s/t_s) ratio of range $50\varepsilon^2$ - $70\varepsilon^2$. The design compression resistance of the unstrengthened steel CHS can be calculated by,

$N_u = A_s f_{ys}$ (cl. 6.2.4) (12)

The design compression resistance of the strengthened steel CHS can be calculated by,

$N_u = A_s f_{ys} + A_{cfrp} f_{cfrp}$ (13)

where $A_{cfrp} = A_r + A_{frp}$; A_r – area of resin; A_{frp} – area of carbon fibre. The predicted strength values are presented in Table 1.

2.3 Australian Standard 4100 [1]

The normalized cross section slenderness parameter λ_s for circular hollow sections is usually expressed in the form

$$\lambda_s = \frac{d^s}{t^s}\frac{\sigma_y^s}{250} \quad (14)$$

Accounting for the equivalent cross section the slenderness parameter λ_{es} is now written in the form

$$\lambda_{es} = \frac{d^{es}}{t^{es}}\frac{\sigma_y^s}{250} \quad (15)$$

Thickness of supplanted section $t_{es} = t_t - t_s$ (16)

Equivalent diameter $d_{es} = d_s + 2\, t_{es}$ (17)

The yield slenderness limit for circular cross section is given by

$$\frac{d_{es}}{t_{es}} \le \left(\frac{250}{\sigma_y^s}\right)82 \quad (18)$$

The section capacity of CHS under axial compression is determined as

$N_u = k_f A_s f_{ys}$ (cl.6.2.1) (19)

The section capacity of the CFRP strengthened CHS under axial compression is determined as

$N_u = k_f A_s f_{ys} + A_{cfrp} f_{cfrp}$ (20)

where

$A_{cfrp} = A_{es} - A_s$ (21)

$A_{es} = A_s [1 + (t_{es} / t_s)]$ (22)

The predicted strength values are presented in Table 1.

Table 1: Axial load carrying capacity in kN

Specimen designation	Eurocode3	AS-4100	AS-4600
HS-CS	256.196	256.196	145.925
HS-30-20-L1	285.163	301.328	172.206
HS-30-20-L2	307.906	331.088	195.9674
HS-30-20-L3	318.42	360.847	209.289
HS-50-40-L1	285.163	301.328	172.206
HS-50-40-L2	307.906	331.088	195.9674
HS-50-40-L3	318.42	360.847	209.289
HS-100-100-L1	285.163	301.328	172.206
HS-100-100-L2	307.906	331.088	195.9674
HS-100-100-L3	318.42	360.847	209.289

3. MATERIALS

3.1 Carbon Fibre

The CFRP used is a low modulus carbon fibre from the MBrace family named as Mbrace CF240, with an elastic modulus of 240 kN/mm^2 and an ultimate tensile strength of 3800 N/mm^2. The fibre is unidirectional with thickness of 0.234mm and width of 500mm. It is fabric type and can be tailored into any desired shape.

3.2 Resin Matrix

The Mbrace Saturant supplied by BASF India Inc was used in this study to provide necessary bonding between steel tube and carbon fibre. It is a two part system, a resin base and a hardener and the mixing ratio was 100:40 (B: H).

3.3 Circular Steel

The circular hollow steel tube confirming to IS 1161:1998 were used in this study. The diameter and thickness considered was 219.7mm and 4.0mm respectively. The yield strength of CHS is 250N/mm^2.

4. EXPERIMENTAL INVESTIGATION

4.1 Strengthening of Specimens

Totally ten specimens of 2.0mm thick and 165.1mm diameter were used. The tube dimensions were chosen so that the D/t ratio was within the range of $70\varepsilon^2$-$90\varepsilon^2$. The 500mm long circular hollow steel tubes were cut from the 6m long tubes. Sand blasting was carried out on the surface of the steel substrate to make the surface rough enough. Then acetone was used to remove the corroded particles and to prepare the surface for wrapping of FRP fabrics. Then the resin matrix was prepared based on the manufacturer's instructions with the ratio 100:40 and mixed thoroughly. The prepared resin matrix was then applied on the steel surface evenly without any air bubbles. Prior to CFRP wrapping and to avoid galvanic corrosion, a thin layer of glass fibre fabrics has been wrapped on specimens. The continuous CFRP fabrics were cut into 30mm, 50mm and 100mm wide strips and wrapped with 20mm, 40mm and 100mm spacing respectively. The strengthened specimens were designated as HS-30-20-L1, HS-30-20-L2, HS-30-20-L3 HS-50-40-L1, HS-50-40-L2, HS-50-40-L3, HS-100-100-L1, HS-100-100-L2 and HS-100-100-L3. At the end, L1, L2, and L3 represent wrapping of fibre in transverse direction with one, two and three layers. The control specimen was designated as HS-CS.

4.2 Testing of Specimens

All the tests were executed on a 2000 kN capacity column tester. The specimens were positioned on the testing machine and load was applied to the specimens directly. The load set up is shown in Fig. 1. A linear variable displacement transducer (LVDT) was used to measure the axial deformation of the columns. The load-cell of 2000 kN and the LVDT were connected to a 16-channel data logger to read and store the observations. All the test specimens were loaded to failure. The failure modes, ultimate failure load and the axial deformation were noted for each column.

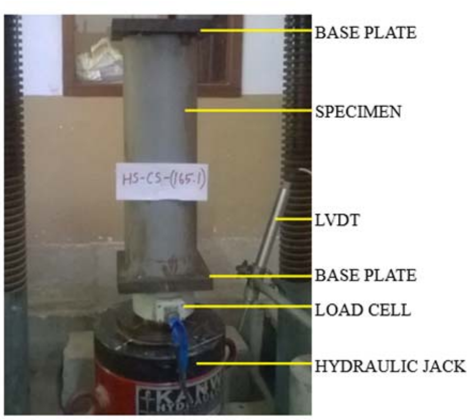

Fig. 1: Experimental Setup

5. RESULTS AND DISCUSSION

5.1 Failure Modes

The control column HS-CS (failed at 225kN) exhibited a distinctive buckling failure i.e. elephant's foot buckling which is proved as common failure mode in hollow steel tubes as in the past researches and it was observed at different levels for different specimens. In the case of strengthened specimens such as HS-30-20-L1 and HS-50-40-L1, the failure was similar because of the close spacing of CFRP strips. In both the specimens, the failure was dominated by outward buckling of the steel tubes near the top end and unwrapped area with the fibre crushing sound at the respective loads of 298 kN and 297 kN. But in case of HS-100-100-L1 specimen the failure was initiated by outward buckling at both top and bottom spacing simultaneously at the load of 250 kN. This was due to the large spacing between the CFRP strips.

Multiple folds were obsered in HS-30-20-L2 and HS-30-20-L3 specimens. This was because of the fact that they sustained more load before failure. The failure of the specimen HS-30-20-L2 was dominated by outward buckling of steel tube near the top end unwrapped zone and also at the middle unwrapped area with the crushing sound of fibre at the respective load of 318 kN. But the specimen HS-30-20-L3 failed by inward buckling of steel tube near the top end unwrapped zone and also at the bottom end unwrapped area with the fibre crushing sound at the load of 293 kN. The failure of specimens such as HS-50-40-L2 and HS-50-40-L3 specimens was observed at the bottom end unwrapped area. The specimen HS-50-40-L2 failed by outward buckling of steel tube near the bottom end unwrapped area with the fibre crushing sound at the load of 309 kN. But in the case of other specimen, the failure was dominated by inward buckling of steel tube near the bottom end unwrapped area with the fibre crushing sound at the respective load of 286 kN.

Fig. 2. Failure mode of HS-CS

In the case of specimens HS-100-100-L2 and HS-100-100-L3, the bulge formation was observed at the top and bottom unwrapped area with the huge crushing sound at the respective load of 290 kN and 277 kN. Due to the external confinement provided by CFRP strips and with the closed spacing, the outward buckling was completely arrested in case of specimens HS-30-20-L3 and HS-50-40-L3 and it enabled the inward buckling of the steel tube. But the inward buckling was not evident in case of HS-100-100-L3 specimen which might be due to large spacing between the CFRP strips. The failure modes of control specimen is shown in Fig. 6.1 and strengthened specimens such as HS-30-20, HS-50-40 and HS-100-100 are shown in Figs 2 to 5 respectively.

Fig. 3: Failure mode of HS-30-20 specimens

Fig. 4: Failure mode of HS-50-40 specimens

Fig. 5: Failure mode of HS-100-100 specimens

5.2 Load Carrying Capacity

The results such as ultimate load and the percentage increase in it are given in Table 2. By strengthening using CFRP, it helped to increase the load carrying capacity of short HSS tubular members (under class3) upto 41%. HS-30-20 specimens showed an increase in axial strength in the range of 30% to 41% while HS-50-40 specimens showed an increase in axial strength between 27% to 32% and the range was about 11% to 29% in case of HS-100-100 specimens when compared to control specimen. In addition, the columns wrapped with two layers showed the maximum increase in axial strength which was about 41%, 37% and 29%, in case of specimens HS-30-20-L3, HS-50-40-L3 and HS-100-100-L3 respectively.

Single layer wrapped specimens showed an increase in axial strength in the range of 11% to 32% while the range is about 23% to 30% in case of three layers wrapped specimens. As the number of layers increases, the confinement effect to control outward buckling was also increased and hence the stress concentration was predominant at the unstrengthened space between the CFRP strips. As a result, the failure of the strengthened specimens was observed at the space between the strips. In addition, the contribution of fibre for increasing the strength was more in case of three layers wrapped specimens, but due to inward buckling of steel tubes, there was decrease in axial strength observed.

Also, the percentage increase in axial strength was more for HS-30-20 and HS-50-40 specimens when compared to HS-100-100 specimens which was due to the effect of closed spacing of CFRP strips. The comparison of ultimate load for the specimens with one layer, two layers and three layers of CFRP strips is shown in Fig 6.

5.3 Deformation Control

The results such as axial deformation and percentage reduction in deformation are given in Table 3. From the results, it can be seen that, by increasing number of CFRP layers, it helped to increase the control of deformation upto 52%. From the experimental results, it was evident that the deformation control was much greater in case of HS-30-20 specimens which is upto 52% whereas it is about 31% and 18% for HS-50-40 and HS-100-100 specimens respectively and the reason might be due to less spacing between the CFRP strips.

The comparison graph of load Vs deformation for all the specimens is shown in Fig 7. The HS-30-20 specimens showed an increase in deformation control in the range of 20% to 52% while the range was about 11% to 31% for HS-50-40 specimens and the range was about 3% to 18% for HS-100-100 specimens. Deformation control was very less in case of HS-100-100 specimens which was due to large spacing between the CFRP strips.

Table 2: Comparison of load carrying capacity

Specimen designation	Semi-Compact section	
	Ultimate load (kN)	% increase in ultimate load
HS-CS	225	-
HS-30-20-L1	298	32.44
HS-30-20-L2	318	41.33
HS-30-20-L3	293	30.22
HS-50-40-L1	297	32

HS-50-40-L2	309	37.33
HS-50-40-L3	286	27.11
HS-100-100-L1	250	11.11
HS-100-100-L2	290	28.88
HS-100-100-L3	277	23.11

Table 3: Comparison of deformation control

Specimen designation	Semi-Compact section	
	Deformation at the failure load of control specimen(mm)	% reduction of axial deformation
HS-CS	4.79	-
HS-30-20-L1	3.85	19.62
HS-30-20-L2	2.97	37.99
HS-30-20-L3	2.32	51.57
HS-50-40-L1	4.26	11.06
HS-50-40-L2	3.84	19.83
HS-50-40-L3	3.32	30.69
HS-100-100-L1	4.65	2.9
HS-100-100-L2	4.28	10.65
HS-100-100-L3	3.93	17.95

5.4 Evaluation of Analytical Results

From the test results, it has been found that there exists a good agreement between theoretical and experimental values of ultimate axial strength in case of Eurocode 3 when compared to AS/NZS 4600 and AS 4100. Eurocode 3 showed variation less than 15% while the variation was upto 30% and 42% in case of AS 4100 and AS/NZS 4600 respectively. The comparison of results obtained through analytical and experimental results is given in Table 4 and also shown in Fig. 8.

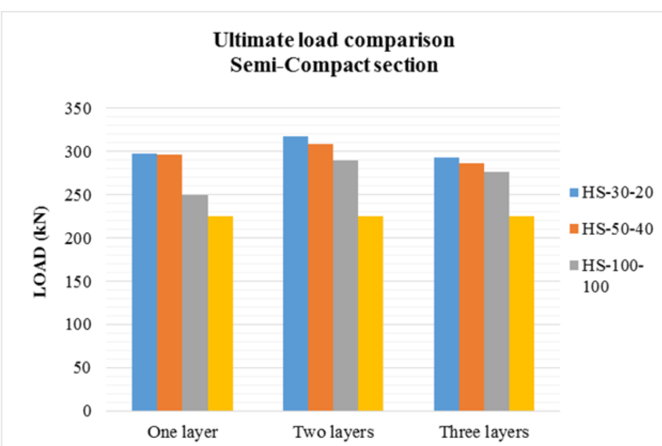

Fig. 6: Ultimate load Comparison

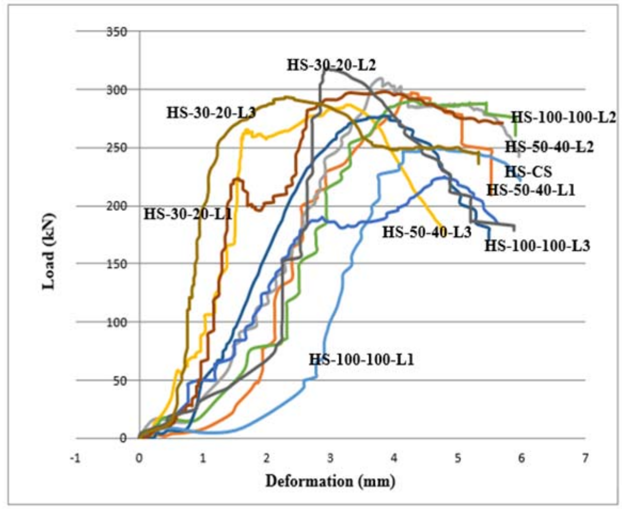

Fig. 7: Load vs Deformation – Comparison

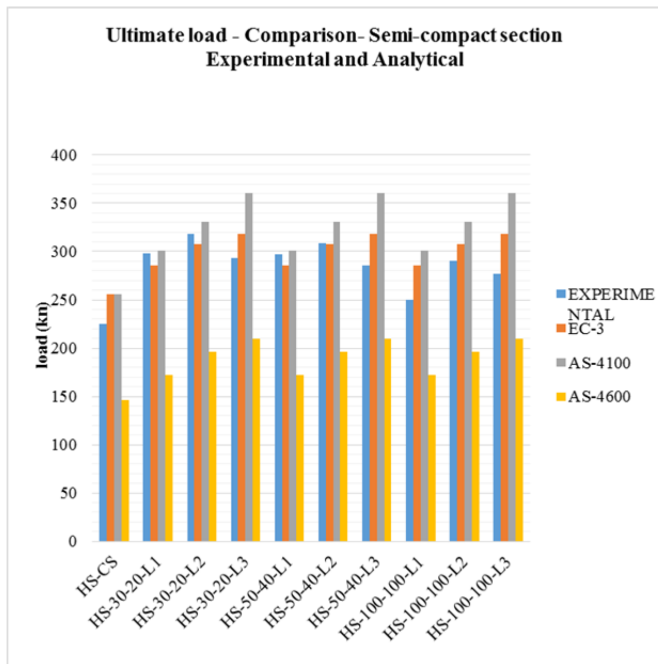

Fig. 8: Ultimate Load – Comparison Experimental and Analytical

6. CONCLUSION

- It was found that CFRP as an external reinforcing material can significantly increase the axial capacity as well as deformation control of CHS columns.

Table 4: Variation in load carrying capacity Analytical results to Experimental results

Specimen designation	Eurocode 3 % ↑ Or % ↓ in load carrying capacity	AS-4100 % ↑ Or % ↓ in load carrying capacity	AS-4600 % ↑ Or % ↓ in load carrying capacity
HS-CS	13.86(↑)	13.86(↑)	35.14(↓)
HS-30-20-L1	4.31(↓)	1.12(↑)	42.21(↓)
HS-30-20-L2	3.17(↓)	4.12(↑)	38.38(↓)
HS-30-20-L3	8.68(↑)	23.16(↑)	28.57(↓)
HS-50-40-L1	3.99(↓)	1.46(↑)	42.02(↓)
HS-50-40-L2	0.35(↓)	7.15(↑)	36.58(↓)
HS-50-40-L3	11.34(↑)	26.17(↑)	26.82(↓)
HS-100-100-L1	14.06(↑)	20.53(↑)	31.12(↓)
HS-100-100-L2	6.17(↑)	14.17(↑)	32.43(↓)
HS-100-100-L3	14.95(↑)	30.27(↑)	24.44(↓)

- The failure mode of all CFRP wrapped specimens occurred in a typical manner of outward ring buckling observed near the ends of specimen, which is commonly known as elephant's foot buckling.
- The HS-30-20 specimens showed an increase in axial strength in the range of 30% to 41% while HS-50-40 specimens showed an increase in axial strength in the range of 27% to 32% and the range was about 11% to 29% in case of HS-100-100 specimens when compared to control specimen.
- The deformation control was much greater in case of HS-30-20 specimens, which is upto 52%, whereas, it is about 31% and 18% for HS-50-40 and HS-100-100 specimens respectively.
- By increasing the spacing between CFRP strips, it decreases the axial capacity of the strengthened specimens and also reduces the deformation control.
- From the analytical results, it is found that Eurocode 3 gives better results when compared to AS/NZS 4600 and AS 4100.
- Eurocode 3 showed variation less than 15% while the variation was upto 30% and 42% in case of AS 4100 and AS/NZS 4600 respectively.
- Further research works necessary to study the effect of inward buckling.

REFERENCES

[1] AS 4100, Steel Structures, Standards Australia, Sydney, 1998.

[2] AS/NZS 4600, Australian/New Zealand Standard, Cold-formed Steel Structures, Standards Australia, Sydney, 2005.

[3] Eurocode 3: Design of steel structures – part 1-1: General rules and rules for buildings, EN 1993 -1-1; 1992, European committee for standardization, Brussels (Belgium): CEN; 2005.

[4] Jagtap P.R., Pore S.M. and Vipul Prakash (2015), 'Necessity of Strengthening of Steel Structures with FRP Composites: a Review', *International Journal of Latest Trends in Engineering and Technology (IJLTET),* Vol.5, No.4, pp. 390-394.

[5] Lelli Van Den Einde, Lei Zhao and Frieder Seible (2003), 'Use of FRP composites in civil structural applications', *Construction and Building Materials,* Vol.17, pp. 389-403.

[6] Mina Dawood, Emmett Sumner and Sami Rizkalla (2006), 'Fundamental characteristics of new high modulus CFRP materials for strengthening steel bridges and structures', *Advances in Engineering Structures, Mechanics and Construction,* pp.215-226.

[7] Priyadarshni M. and Sundarraja M.C. (2016), "Investigation on Axial Behaviour of HSS Tubular Members Strengthened using CFRP", *International Conference on Concrete Vision for Humanity (ICCVH 16)*, March 18, 2016, Ranganathan Engineering College, Coimbatore.

[8] Vaibhav B. Chavan, Vikas N. Nimbalkar and Abhishek P. Jaiswal (2014), 'Economic Evaluation of Open and Hollow Structural Sections in Industrial Trusses', *International Journal of Innovative Research in Science, Engineering and Technology*, Vol.3, No.2, pp.9554-9565.

[9] Viveka V., Shanmugavalli B. and Sundarraja M.C. (2014), 'Analytical Investigation on the Compressive Behaviour of CHS Tubular Columns Strengthened Using FRP Composites', *International Journal of Innovative Research in Science, Engineering and Technology*, Vol. 3, No.1, pp.1582-1585.

[10] Wardenier, J. (2001), *Hollow sections in structural applications*, Delft University of Technology, Netherlands.